

Arachidonoyl-phosphatidylcholine oscillates during the cell cycle and counteracts proliferation by suppressing Akt membrane binding

Andreas Koeberle^{a,b,1}, Hideo Shindou^c, Solveigh C. Koeberle^d, Stefan A. Laufer^e, Takao Shimizu^{b,c}, and Oliver Werz^a

^aDepartment of Pharmaceutical/Medicinal Chemistry, Institute of Pharmacy, Friedrich-Schiller-University, 07743 Jena, Germany; ^bDepartment of Biochemistry and Molecular Biology, Faculty of Medicine, University of Tokyo, 113-0033 Tokyo, Japan; ^cDepartment of Lipid Signaling Project, National Center for Global Health and Medicine, 162-8655 Tokyo, Japan; ^dMorrison Laboratory, Leibniz Institute of Age Research-Fritz-Lipmann-Institute, 07745 Jena, Germany; and ^eDepartment of Pharmaceutical Chemistry, Institute of Pharmacy, University of Tübingen, 72076 Tübingen, Germany

Edited* by Bengt Samuelsson, Karolinska Institutet, Stockholm, Sweden, and approved December 31, 2012 (received for review October 8, 2012)

The activity of protein kinase B (Akt)—a major kinase promoting cell proliferation and survival—oscillates during the cell cycle. To investigate whether membrane phospholipids may regulate Akt phosphorylation and thus activity, we monitored the lipid profile of nocodazole-synchronized mouse NIH 3T3 fibroblasts during the cell cycle by liquid chromatography electrospray ionization tandem mass spectrometry (LC-MS/MS). The proportion of *sn*-2-arachidonoyl-phosphatidylcholine (20:4-PC) inversely correlated with Akt activity. Increasing the cellular ratio of 20:4-PC by supplementation of 20:4-PC to the cell culture medium diminished Akt [serine (Ser)473] phosphorylation. Saturated and monounsaturated phosphatidylcholines, used as control had no effect; 20:4-PC reduced cell proliferation relative to controls, interfered with S-phase transition, and suppressed Akt downstream signaling and cyclin expression like LY294002, which is a specific inhibitor of the phosphatidylinositol-3-kinase/Akt pathway. Additive effects of 20:4-PC and LY294002 were not observed, underlining the critical role of Akt for 20:4-PC signaling; 20:4-PC suppressed Akt membrane translocation as shown by immunofluorescence microscopy but left the concentration of the anchor lipid phosphatidylinositol-3,4,5-trisphosphate unchanged. An *in vitro* binding assay suggests that 20:4-PC attenuates the interaction of Akt with its membrane binding site. We conclude that 20:4-PC oscillates during the cell cycle and delays cell cycle progression by inhibiting Akt membrane binding.

arachidonic acid | lipidomics | protein kinase | cellular signaling | bioactive lipid

The serine/threonine kinase Akt (protein kinase B) is a key regulator of cell proliferation, survival, and metabolism (1) and is critically involved in multiple other processes (e.g., immunomodulation) (2). Dysregulation of Akt is associated with diverse diseases including cancer, cardiovascular disorders, and diabetes (1, 3). Activation of Akt requires membrane translocation to phosphatidylinositol-3,4,5-trisphosphate (PIP₃) binding sites and phosphorylation at [threonine (Thr)308] and [serine (Ser)473] by corecruited kinases (1). Phosphorylated and activated Akt dissociates from the membrane and initiates multiple downstream signal transduction pathways (1). Among the substrates of Akt are regulators of the cell cycle, protein biosynthesis, apoptosis, and metabolism (1, 3). Inhibition of basal Akt signaling reduces cyclin expression and delays cell cycle progression (4–6). The phosphorylation state of Akt (Ser473) oscillates during the cell cycle (4). Highest levels of phosphorylated and thus activated Akt were found during the G2/M-phase in diverse cell lines (4, 5, 7). Although intensively investigated, the molecular mechanisms underlying the oscillation of Akt activity remain obscure. Because Akt is recruited to membranes for activation (1), we speculated that Akt activity might be regulated by an oscillating membrane lipid component.

Phospholipids (PLs) form the bilayer of biomembranes and consist of a glycerol backbone, two esterified fatty acids, and

a polar head group (8). The head group defines the PL subclass: phosphatidylcholine (PC), phosphatidylethanolamine (PE), phosphatidylserine (PS), phosphatidylinositol (PI), or phosphatidylglycerol (PG). Fatty acid compositions of PLs are matured by lysophospholipid (LPL) acyltransferases through the Lands cycle (9). PLs are synthesized during the G1- and S-phase of the cell cycle and are essential for cell cycle progression (10). Disturbed PL biosynthesis results in cell cycle arrest and apoptosis (8, 10). An essential role of PLs in cell cycle regulation has been confirmed by numerous studies (8, 10–12), but the function of individual PL species is largely unknown due to the lack of comprehensive lipidomic studies.

Here, we applied liquid chromatography electrospray ionization tandem mass spectrometry (LC-MS/MS) to monitor the PL profile during the cell cycle of mouse NIH 3T3 fibroblasts. The proportion of *sn*-2-arachidonoyl-phosphatidylcholine (20:4-PC) strongly increased during the G1-phase of the cell cycle and inversely correlates with previously reported Akt activity (4, 5, 7). We further show that 20:4-PC delays cell cycle progression and cell proliferation and ascribe the antiproliferative effect of 20:4-PC to an inhibition of Akt membrane translocation and subsequent signaling. Together, our study implies a role of 20:4-PC in triggering Akt activity during the cell cycle.

Results

Proportion of Arachidonoyl (20:4)-PC Increases During G1-Phase of the Cell Cycle. The activity of various key enzymes involved in cell proliferation and survival oscillates during the cell cycle, but the underlying mechanisms are not fully understood. Among them is the serine/threonine kinase Akt whose activity peaks during the G2/M-phase of the cell cycle (4, 5, 7). To identify those membrane lipids that might interfere with regulators of the cell cycle (particularly Akt), we monitored the PL profile of synchronized NIH 3T3 mouse fibroblasts during cell cycle progression by LC-MS/MS. Cells were synchronized with the anti-microtubule agent nocodazole in the G2/M-phase and then released into a new cell cycle. We followed cell cycle progression by propidium iodide staining of DNA (which duplicates during the cell cycle) and flow cytometry. Synchronized cells rapidly passed mitosis after removal of nocodazole (<1 h), stayed in the G1-phase up to 11 h, proceeded to S-phase (11–21 h), and reentered the G2/M-phase (>14 h; Fig. S1). Synchronization was lost for cultivation longer than 21 h. The amount of cellular PLs halved during

Author contributions: A.K., T.S., and O.W. designed research; A.K. performed research; S.C.K., S.A.L., T.S., and O.W. contributed new reagents/analytic tools; A.K. and H.S. analyzed data; and A.K., H.S., S.C.K., T.S., and O.W. wrote the paper.

The authors declare no conflict of interest.

*This Direct Submission article had a prearranged editor.

¹To whom correspondence should be addressed. E-mail: andreas.koeberle@uni-jena.de.

This article contains supporting information online at www.pnas.org/lookup/suppl/doi:10.1073/pnas.1216182110/-DCSupplemental.

cell division and recovered during the G1-phase (Fig. S2A), as reported (13). Differences were observed between PL species. Thus, during the G1-phase, the proportion of *sn*-2 20:4-containing PC species {PC[palmitic acid (16:0)/20:4], PC[palmitoleic acid (16:1)/20:4], PC[stearic acid (18:0)/20:4]/PC[oleic acid (18:1)/eicosatrienoic acid (20:3)], PC(18:1/20:4) (Fig. S2 B and C), and polyunsaturated ether PC species (Table S1)} increased relative to species with monounsaturated fatty acids [PC(16:0/16:1), PC(18:1/16:1), PC(16:0/18:1), and PC(18:1/18:1)] (Fig. 1A; Fig. S2B). The accumulation of 20:4-PC was accompanied by an increased ratio of the related LPL 20:4-LPC (Fig. 1A). Moreover, 20:4 was also enriched in less abundant PLs such as PG, PS, and PI (but not in PE) during the S-phase (Fig. 1B).

20:4-PC Interferes with Cell Cycle Progression. To investigate the effect of 20:4-PC on cell cycle progression, we supplemented the 20:4-containing PC species PC(16:0/20:4) and PC(18:0/20:4) (purity: >99%) to the cell culture medium and cultivated the cells for 48 h. PC[heptadecanoic acid (17:0)/17:0], PC(16:0/18:1), PC[16:0/linoleic acid (18:2)], and a crude mixture of egg PC species (rich in 16:0, 18:1, and 18:2) were used as controls to recognize PC-dependent effects not related to the fatty acid composition. Both PC(16:0/20:4) and PC(17:0/17:0) were incorporated into cells as confirmed by LC-MS/MS, although PC(17:0/17:0) was more strongly enriched after 48 h (Fig. S3A). FCS—a routine additive to the cell culture medium—was charcoal-stripped to reduce its PL concentration (Fig. S3 B and C), which might otherwise reduce the responsiveness of the cells to exogenously added PLs. Charcoal-stripping of FCS reduced the proliferation rate (=cell number) of NIH 3T3 cells 2.6-fold ($n = 4$), similar to serum deprivation (14). Supplementation with PC(17:0/17:0) concentration-dependently restored the proliferation rate (Fig. 2A). PC(16:0/18:1), PC(16:0/18:2), and crude egg PC were less efficient (Fig. S3D). The 20:4-containing PC species PC(16:0/20:4) and PC(18:0/20:4) seem to have dual effects on proliferation (Fig. 2A; Fig. S3D). Thus, cell proliferation was partially restored at a low PC(16:0/20:4) concentration (4 μ M) (Fig. 2A), whereas increasing concentrations of PC(16:0/20:4) or PC(18:0/20:4) (40–120 μ M) reduced the proliferation rate again to the basal level (Fig. 2A; Fig. S3D). The enhanced cell proliferation due to PC(17:0/17:0) was blocked by cotreatment with PC(16:0/20:4) (120

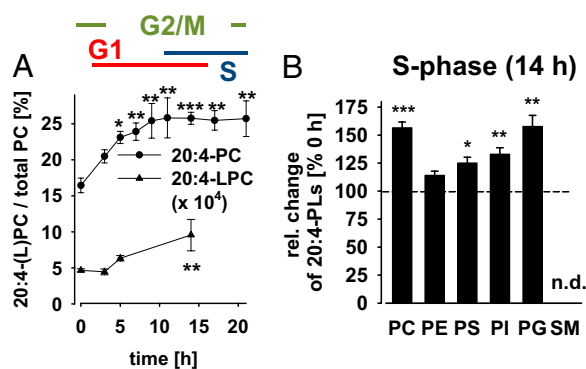


Fig. 1. 20:4-PC accumulates during the G1-phase of the cell cycle. NIH 3T3 cells (4×10^6 cells/10-cm dish) were synchronized by nocodazole (0 h) and released into a new cell cycle. Relative intensities of PL and LPC species were determined by LC-MS/MS. (A) Signal intensities of 20:4-containing PC and LPC species relative to total PC intensity. (B) Change of 20:4-containing PLs in the S-phase relative to the G2/M-phase (14 vs. 0 h after removal of nocodazole); 100% corresponds to relative intensities of $16.4 \pm 1.0\%$, $31.9 \pm 0.6\%$, $8.0 \pm 0.5\%$, $21.3 \pm 1.6\%$, and $7.14 \pm 0.5\%$ for 20:4-PC, -PE, -PS, -PI, and -PG, respectively. Sphingomyelins (SMs) containing 20:4 were not detectable (n.d.). Data are given as means \pm SEM; $n = 3-6$. * $P < 0.05$, ** $P < 0.01$, *** $P < 0.001$ vs. G2/M-phase (0 h); ANOVA + Tukey HSD post hoc tests.

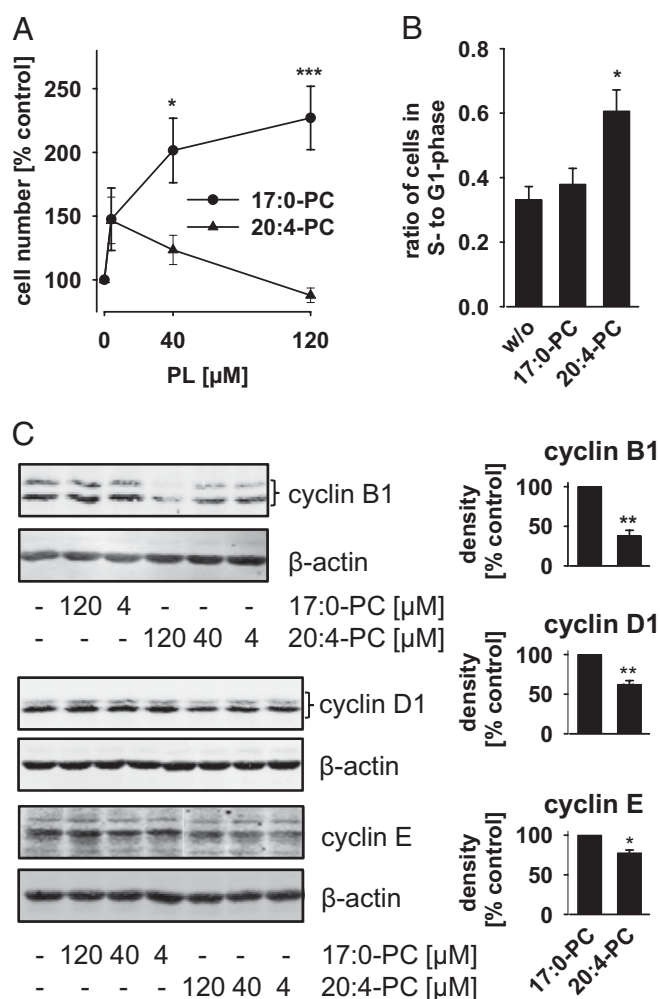


Fig. 2. 20:4-PC interferes with cell cycle progression. NIH 3T3 cells (1.2×10^6 /75-cm² flask) were treated for 48 h with or without PC(17:0/17:0) (17:0-PC) or PC(16:0/20:4) (20:4-PC) (120 μ M, each, or as otherwise indicated) in DMEM supplemented with 10% charcoal-stripped FCS. (A) Cell numbers were determined after trypan blue staining using a Vi-CELL Series Cell Counter (Beckman Coulter). (B) Cell cycle distribution was analyzed by propidium iodide staining and flow cytometry. See Fig. S3F for histogram plots. (C) Expression of cyclin B1, D1, and E was analyzed at the protein level by Western blot. β -Actin expression was determined as control. (Right) Data from densitometric analysis. Data are given as means \pm SEM; $n = 3-10$. * $P < 0.05$, ** $P < 0.01$, *** $P < 0.001$ vs. the untreated control (A and B) or 17:0-PC-treated control (C); ANOVA + Tukey HSD post hoc tests (A and B) and Student *t* test (C). Western blots are representative of three independent experiments (B).

μ M each; Fig. S3D). Cell viability was not decreased as determined by trypan blue staining, excluding acute cytotoxic or proapoptotic effects (Fig. S3E).

Propidium iodide staining and flow cytometric cell cycle analysis revealed that PC(16:0/20:4) increased the ratio of cells in the G1- to S-phase (Fig. 2B; Fig. S3F). Such an increase was recently reported for the selective PI3K inhibitor LY294002 after short-term treatment (3 h) of NIH 3T3 cells (4). Cell cycle-dependent events are triggered by cyclins (15) whose expression is regulated by key mediators of cell proliferation and survival (including Akt) (16). In fact, PC(16:0/20:4) significantly inhibited the expression of cyclin B1 and less of other cyclins as determined by Western blotting (Fig. 2C).

20:4-PC Inhibits Akt Signaling. To elucidate how 20:4-PC attenuates cell cycle progression, we investigated its effect on key signaling

pathways of cell proliferation and survival through analyzing protein expression and phosphorylation by Western blot. Among the relevant proteins analyzed were ERK, PKC, Src, Akt, p38-MAPK, JNK, NF- κ B, and caspase 3 (Fig. 3A; Fig. S4A). PC(16:0/20:4) concentration- ($\geq 40 \mu\text{M}$; Fig. 3A) and time-dependently ($\geq 1 \text{ h}$; Fig. 3B) inhibited the basal phosphorylation of the mitogenic protein kinase Akt, prevented insulin-induced Akt phosphorylation (Fig. 3C), and decreased the phosphorylation of the Akt substrate p70S6 kinase (Fig. 3A). The ability of PC to suppress Akt phosphorylation decreased from 20:4-containing PC(16:0/20:4) and PC(18:0/20:4) to di-unsaturated PC(16:0/18:2) and was not evident for

monounsaturated PC(16:0/18:1) and saturated PC(17:0/17:0) (Fig. S4B). Moreover, PC(16:0/20:4) enhanced the phosphorylation of the antiproliferative and apoptosis-inducing p38-MAPK (at $120 \mu\text{M}$) (Fig. 3A). Phosphorylation of ERK, MARCKS (PKC substrate), Src, and JNK was not affected (Fig. S4A). Akt and p38-MAPK pathways are apparently independently modulated by PC(16:0/20:4) because specific inhibition of PI3K/Akt signaling by LY294002 failed to increase p38-MAPK phosphorylation (Fig. S4C), and specific inhibition of p38-MAPK by Skepinone-L [visualized by reduced heat shock protein (HSP)-27 phosphorylation, Fig. S4D] (17) could not recover phospho-Akt levels in PC(16:0/20:4)-treated cells (Fig. S4E).

It seemed reasonable to speculate that supplemented 20:4-PC decreases cell proliferation through inhibition of Akt signaling. To prove this hypothesis, cyclin B1 and D1 were used as marker for cell cycle progression (18). If 20:4-PC acts on cell proliferation predominantly by inhibiting Akt signaling, a specific inhibitor of PI3K/Akt signaling should decrease cell cycle progression to a similar extent, and coaddition of 20:4-PC should have no further effect. In fact, the specific PI3K inhibitor LY294002 reduced cyclin B1 and D1 expression (Fig. 3D) like 20:4-PC (Fig. 2C), and the combination showed no additive effects (Fig. 3D). Specific inhibition of p38-MAPK by Skepinone-L did not affect cyclin expression (Fig. S4F). In summary, our data indicate a correlation between 20:4-PC and cell proliferation (Fig. 2A) related to Akt phosphorylation (Fig. 3A).

20:4-PC has been supplemented to the cell culture medium for all studies this far. Endogen turnover of 20:4-PC essentially depends on lysophospholipid acyltransferases (9, 19) and phospholipases A_2 (20, 21). Cytosolic phospholipase $A_2\alpha$ degrades PLs by hydrolyzing the *sn*-2 fatty acid ester, has specificity for 20:4-PC (20), and is abundantly expressed in an activated (=phosphorylated) state in NIH 3T3 cells (Fig. S4G). This isoenzyme was specifically inhibited by pyrrolidine-1 to impair 20:4-PC degradation. In fact, pyrrolidine-1 significantly decreased the phosphorylation of Akt (Fig. 3E) as expected. Bromoenol lactone—an inhibitor of Ca(II)-independent PLA $_2$, which is not specific for inhibition of 20:4-PC hydrolysis (22)—was used as control and did not significantly reduce phospho-Akt levels (Fig. 3E).

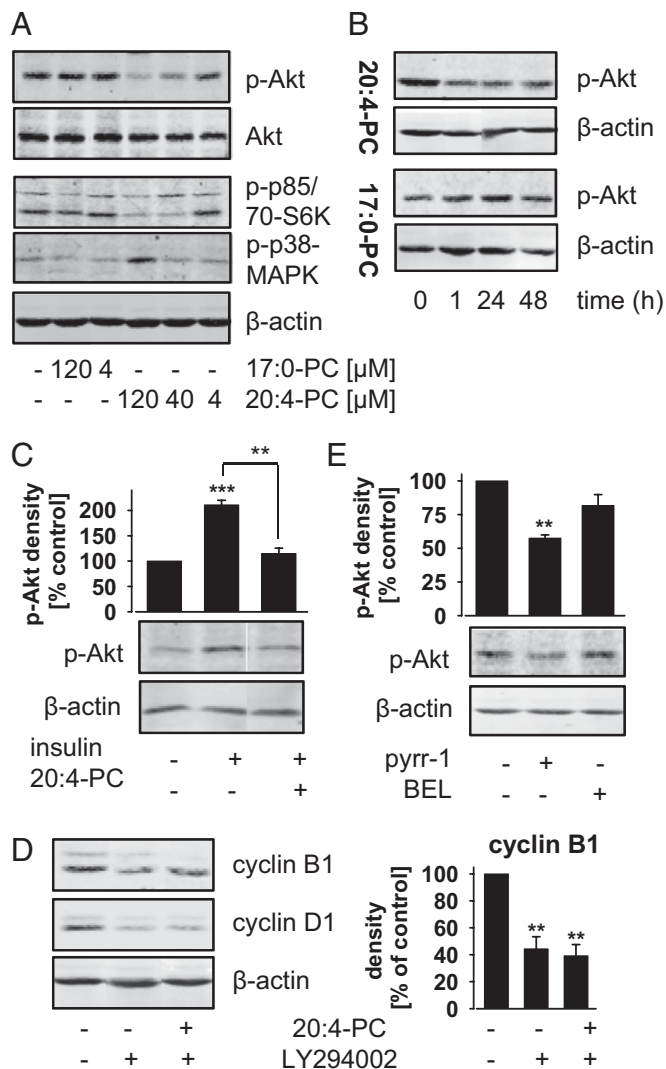


Fig. 3. 20:4-PC inhibits Akt signaling. Protein levels of p-Akt (Ser473), Akt, p-p70S6 kinase (p-p70S6K, Thr389; lower band), p-p85S6K (upper band), cyclin B1 and D1, and β -actin were determined by Western blot. (A and B) NIH 3T3 cells were treated as described in Fig. 2. Concentration- (A) and time-dependent effects (B) of PC(17:0/17:0) (17:0-PC) and PC(16:0/20:4) (20:4-PC) ($120 \mu\text{M}$ each or as otherwise indicated). (C) Confluent cells were treated with or without 20:4-PC ($120 \mu\text{M}$) in DMEM plus 0.2% BSA for 24 h and then stimulated with insulin ($2 \mu\text{M}$) for 15 min. (D and E) NIH 3T3 cells ($5 \times 10^5/25\text{-cm}^2$ flask) were treated with 20:4-PC ($120 \mu\text{M}$) and/or vehicle (DMSO), LY294002 ($10 \mu\text{M}$), pyrrolidine-1 (pyrr-1; $2.5 \mu\text{M}$) or bromoenol lactone (BEL; $10 \mu\text{M}$) for 48 h in DMEM plus 10% charcoal-stripped FCS. (C–E) Blots were densitometrically analyzed. Data are given as means \pm SEM; $n = 3$. $**P < 0.01$, $***P < 0.001$ vs. the untreated control; ANOVA + Tukey HSD post hoc tests. Western blots are representative of two to three independent experiments.

20:4-PC Suppresses Akt Signaling by Inhibiting Akt Membrane Binding. Release of 20:4 from 20:4-PC may initiate eicosanoid biosynthesis (21). Hence, we investigated whether a disturbed eicosanoid formation might underlay the effect of 20:4-PC on cell proliferation. In 20:4-PC-treated cells ($120 \mu\text{M}$, 48 h), the cellular amount of free 20:4 was not changed (Fig. S5A), and eicosanoid levels [e.g., prostaglandin (PG) E_2 , PGD $_2$, PGF $_{2\alpha}$, and leukotriene (LT)B $_4$] remained below the detection limit as determined by LC-MS/MS. Moreover, supplementation of 20:4 failed to inhibit Akt phosphorylation (Fig. S5B), and PGE $_2$ (one of the major prostaglandins formed by activated 3T3 fibroblasts; ref. 23) did not reduce NIH 3T3 cell proliferation (Fig. S5C). Caution should be used when interpreting data based on exogenous 20:4, which might not only be metabolized to eicosanoids but also incorporated into PC and other PLs (24). Along these lines, inhibitors of prostaglandin and leukotriene formation (i.e., indomethacin and BWA4C) could not abolish the differences in proliferation between cells treated with PC(16:0/20:4) or PC(17:0/17:0) (Fig. S5D). These data suggest that the antiproliferative effect of 20:4-PC is neither mediated by 20:4-PC-derived free 20:4 nor eicosanoids.

Next, we analyzed whether 20:4-PC interferes with Akt translocation by immunofluorescence microscopy. Akt forms membrane-associated clusters in insulin-stimulated NIH 3T3 cells (Fig. 4A) and becomes phosphorylated (Fig. 3C). Both suppression of PIP $_3$ /Akt signaling by LY294002 and supplementation of 20:4-PC inhibited Akt membrane translocation (Fig. 4A). 20:4-PC might directly interfere with Akt membrane

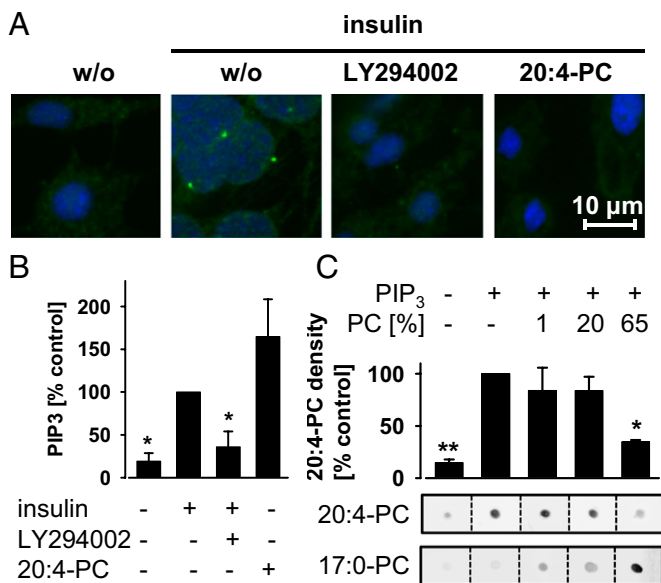


Fig. 4. 20:4-PC inhibits Akt membrane translocation. (A and B) Confluent NIH 3T3 cells were treated with or without PC(16:0/20:4) (20:4-PC; 120 μ M) in DMEM plus 0.2% BSA for 24 h. After preincubation with or without LY294002 (10 μ M) for 10 min, cells were stimulated with insulin (2 μ M) for 15 min. (A) Granule structures of Akt are formed at membranes on stimulation with insulin. Their formation is disturbed by LY294002 or 20:4-PC. Akt was detected by rabbit anti-Akt and visualized using IRDye 800CW goat anti-rabbit. (Scale bar, 10 μ m.) The stains of Akt (green) are representative for three independent experiments and merged with DNA-stains (DAPI, blue). (B) Cellular PIP₃ levels were determined by ELISA; 100% corresponds to 0.3 ± 0.1 nmol PIP₃/mg total protein. (C) Effect of 20:4-PC and PC(17:0/17:0) (17:0-PC) on the binding affinity of Akt to PIP₃. Human recombinant Akt (1 μ g) was spotted onto nitrocellulose and incubated with liposomes of different 20:4-PC or 17:0-PC ratios (PC). Liposomes contained PIP₃ for binding Akt and biotinylated PE for labeling with IRDye 800CW streptavidin. (Lower) Stains are representative of three to four independent experiments. (Upper) Results from the densitometric analysis are presented for the 20:4-PC-labeled stains. Data are given as means \pm SEM; $n = 3-4$. * $P < 0.05$, ** $P < 0.01$ vs. the insulin-stimulated (B) or PIP₃-containing but 20:4-PC-free control (C); ANOVA + Tukey HSD post hoc tests.

binding but could also block upstream signal cascades that regulate PIP₃ levels—the membrane anchors of Akt. Levels of cellular PIP₃ were not decreased but rather increased by 20:4-PC as measured by ELISA (eventually to encounter the suppressed Akt activity; Fig. 4B), suggesting a direct effect of 20:4-PC on Akt membrane binding. In fact, using a cell-free dot blot liposome overlay assay, we observed that an increased ratio of 20:4-PC decreases the binding of Akt to liposomes (consisting of saturated and mono- and diunsaturated PC and PE) with PIP₃ binding sites (Fig. 4C). The control PC(17:0/17:0) enhanced the binding of Akt to liposomes instead (Fig. 4C).

Discussion

Differences in the proportion of 20:4-PLs were previously observed between proliferating and confluent cells and have been associated with cell cycle progression (25). Using LC-MS/MS-based lipidomics, we show that cellular 20:4-containing PL and LPL species oscillate during the cell cycle of NIH 3T3 mouse fibroblasts. Supplemented 20:4-PC prevented membrane translocation of the protein kinase Akt apparently by reducing its affinity to PIP₃ binding sites. As a consequence, phosphorylation (and thus activation) of Akt and downstream signaling (e.g., activation of p70S6 kinase) were inhibited. Impaired Akt signaling correlated with delayed cell cycle progression and reduced cell proliferation (Fig. S6).

The large majority of studies ascribe biological effects of 20:4-PC to the release of 20:4 and the subsequent formation of bioactive eicosanoids (21). Cell proliferation correlates with eicosanoid formation in most of these studies (26). Only few reports discuss antiproliferative effects of 20:4-PC, which are independent of free 20:4 and its conversion to eicosanoids (27). The latter is strongly supported by our study. Thus, supplementation of 20:4-PC did not evoke prominent eicosanoid formation or 20:4 release, and concomitant inhibition of eicosanoid formation could not elevate cell proliferation to the rate reached in presence of the negative control PC(17:0/17:0). Other 20:4 metabolites than prostaglandins and leukotrienes were not addressed by the inhibitor approach. The recruitment of Akt to membranes is generally regulated by receptor-mediated formation or degradation of the Akt anchor molecule PIP₃ (1), and receptors of bioactive 20:4 metabolites (i.e., prostaglandins, leukotrienes, and cytochrome P₄₅₀ products) enhance PIP₃ formation by activating PI3K (21). 20:4-PC inhibited Akt translocation without decreasing cellular levels of PIP₃, again excluding a role of eicosanoid formation for cell proliferation under our experimental conditions. Instead, 20:4-PC reduced the affinity of Akt to PIP₃ binding sites within liposomes in a cell-free assay. These findings might explain why only Akt activity but not PIP₃ levels were found to oscillate during the cell cycle (4). Whether 20:4-PC inhibits Akt translocation by direct interaction with Akt or by modulating membrane properties (e.g., decreasing membrane fluidity; ref. 28) remains elusive. Although eicosanoids (derived from 20:4-PC or other PLs) seem not to affect the proliferation of NIH 3T3 cells under our experimental conditions, they possess well-documented mitogenic activity for many other cell types and various culture conditions (26). 20:4-PC might modulate cell proliferation under these conditions either (i) predominantly by providing 20:4 for eicosanoid formation or (ii) by a combination of enhanced eicosanoid biosynthesis and inhibition of Akt membrane binding. Such an opposing regulation might also exist for other cellular processes related to eicosanoids and Akt signaling, including inflammation and its resolution.

The potency of PC species to suppress Akt signaling decreased with their unsaturation index from polyunsaturated (=20:4-containing) over di-unsaturated to monounsaturated and saturated species (Fig. S4B). The interference with Akt signaling might explain why 20:4-PC failed to induce cell proliferation, but how other PC species affect proliferation remains elusive. PC(17:0/17:0), for example, was most efficient in restoring proliferation of cells grown in lipid-reduced medium but did not change the phosphorylation state of Akt. Biological functions of exogenous PLs might depend on their uptake, subcellular distribution, and turnover. In fact, PC(17:0/17:0) was more strongly enriched in NIH 3T3 cells after 48 h than PC(16:0/20:4) (Fig. S3A). However, uptake, distribution, and metabolism of 20:4-PC to bioactive lipids does not seem essential for inhibiting Akt translocation because 20:4-PC reduced Akt membrane binding in a cell-free system lacking metabolizing enzymes. 20:4-PC metabolites might, however, amplify the antiproliferative effect of 20:4-PC or possess biological functions not related to Akt signaling and proliferation—especially 20:4-LPC, whose proportion increased along with 20:4-PC during the G1-phase of the cell cycle. Unfortunately, 20:4-LPC is not commercially available, and its cellular formation cannot be selectively blocked without detailed understanding of its biosynthesis.

The activity of Akt is well known to oscillate during the cell cycle, but the underlying mechanisms remained obscure despite intensive research (4, 5, 7). 20:4-PC (and related polyunsaturated PLs) might be the missing link that triggers cell cycle progression and Akt signaling. Intriguingly, Akt activity has been reported as being highest during the G2/M-phase (4, 5, 7), when levels of 20:4-PC are lowest (Fig. 1A). Indeed, increasing levels of 20:4-PC suppressed Akt signaling in our study. Whether physiologically occurring oscillations of 20:4-PC (and related PLs) also regulate

Akt activity could not be directly addressed. A direct proof would require the knowledge of isoenzymes involved in cell cycle-dependent 20:4-PC biosynthesis and tools for the specific blockade of 20:4-PC formation. Both are currently not available. The functional relevance of 20:4-PC in the regulation of Akt signaling and cell cycle is, however, supported by indirect studies. Shtivelman et al. (4) could not observe a decrease of Akt activity during the G2/M-phase when NIH 3T3 cells were serum starved and thus depleted of polyunsaturated PLs (including 20:4-PC) (29), and Tercé et al. (11) reported that PC biosynthesis is required for normal cell cycle progression in fibroblasts. Also, a nutritional regulation of the cell cycle by 20:4-PC seems likely. Human blood plasma contains 2.6 mM PLs including 0.5 mM 20:4-containing PC (30). Effects of supplemented 20:4-PC on Akt signaling and cell cycle thus occur at physiologically highly relevant concentrations (40–120 μ M).

Taken together, our study investigated the cellular PL composition during the cell cycle of a mouse fibroblast cell line and found the proportion of 20:4-PC strongly increased during the G1-phase. Supplementation of 20:4-PC reduced cell cycle progression, inhibited Akt signaling, and impaired Akt membrane translocation. 20:4-PC seemingly attenuates the affinity of Akt for binding to PIP₃. Comparable effects on Akt signaling were observed by suppressing the enzymatic degradation of endogenous 20:4-PC. It is tempting to speculate about a role of 20:4-PC for regulating cell cycle progression and mitogenic signaling in hyperproliferative diseases. High levels of 20:4-PLs might, for example, impair uncontrolled cell growth in cancer as 20:4-PC counteracts Akt signaling and thus proliferation. In fact, several lipidomic studies found decreased levels of PLs and LPLs containing 20:4 in blood and tissues of cancer patients (31–35).

Materials and Methods

Materials. PLs and lipid standards were bought from Avanti Polar Lipids. Defined PC species (purity > 99% each) were prepared by Avanti Polar Lipids from *sn*-glycero-3-phosphocholine, which was extracted from soybean lecithin. Aliquots were dissolved in chloroform, protected from light, and stored at –80 °C under argon. Primary antibodies were obtained from Cell Signaling or Santa Cruz Biotechnology. Secondary antibodies and IRDye 800CW-labeled streptavidin were from LI-COR Biosciences. The following materials were used: LY294002 (Cayman); pyrrolidine-1 (Merck); nonactivated human Akt1 (BPS Bioscience); and PC from egg yolk, bromoenol lactone, insulin, and nocodazole (Sigma-Aldrich).

Heat-inactivated FCS was treated with dextran-coated charcoal (20 mg/mL) under rotation for 16 h at 4 °C to lower the concentration of lipophilic components [such as PC(16:0/20:4) and free 20:4; Fig. S3 B and C]. After dextran-coated charcoal was removed by repeated centrifugation (10,000 \times g, 10 min, 4 °C), the supernatant (charcoal-stripped FCS) was sterile filtrated, and aliquots were frozen at –20 °C. Liposomes were formed from PLs by sonication at 40 °C for 20 min and vigorous mixing in DMEM plus 10% charcoal-stripped FCS or DMEM plus 0.2% fatty acid free BSA before supplementation to the cell culture medium.

Cells, Cell Counting, and Cell Cycle Synchronization. Mouse NIH 3T3 fibroblasts were cultivated at 37 °C and 5% CO₂ in DMEM containing 10% (vol/vol) heat-inactivated FCS. Total and viable cells were counted after trypan blue staining using a Vi-CELL Series Cell Counter (Beckman Coulter). For cell cycle synchronization, NIH 3T3 cells (70–80% confluent) were treated with nocodazole (0.4 μ g/mL) in DMEM plus 10% FCS for 20 h at 37 °C and 5% CO₂. Round mitotic cells were detached by rocking and squirting and washed three times with ice-cold PBS, pH 7.4. Synchronized cells were reseeded at 4 \times 10⁶ in DMEM plus 10% FCS on 10-cm culture dishes and cultured for the indicated times at 37 °C and 5% CO₂.

Propidium Iodide Staining and Flow Cytometry. NIH 3T3 cells were harvested by trypsinization, resuspended in PBS (1–5 \times 10⁶) and fixed in 70% (vol/vol) aqueous ethanol. After centrifugation (300 \times g, 5 min), the cell pellet was washed with PBS, suspended in propidium iodide staining solution [1 mL; PBS plus 0.1% (vol/vol) Triton X-100, 50 μ g/mL propidium iodide, 100 μ g/mL DNase-free RNase], and incubated at room temperature for 30 min. Cells were filtered through a mesh filter (BD Biosciences) and analyzed by flow cytometry (EPICS XL; Beckman Coulter). Data were analyzed using MultiCycle

(Phoenix Flow Systems) or Weasel (Walter and Eliza Hall Institute for Medical Research) software.

Extraction of PLs. PLs and LPLs were extracted from cultured cells (5 \times 10⁵) according to the method of Bligh and Dyer (36). PC[myristic acid (14:0)/14:0] and PE(14:0/14:0) (0.4 nmol each) were used as internal standards. The extracted lipids were dissolved in 100 μ L methanol, diluted, and applied to LC-MS/MS analysis.

Reversed Phase LC and MS. Chromatography was carried out on an Acquity UPLC BEH C₈ column (1.7 μ m, 1 \times 100 mm; Waters) using an Acquity Ultra-performance LC system (Waters) as previously described (37). Lipids were detected, and their structure was verified by a TSQ Vantage Triple Stage Quadrupole Mass Spectrometer (Thermo Scientific) equipped with an HESI-II electrospray ionization source as previously described (38) and detailed in *SI Materials and Methods*. In brief, PC and sphingomyelins were quantified as [M+H]⁺ by *m/z* = 184 precursor ion scans in the positive ion mode (collision energy: 35 V). All other PLs (PE, PS, PI, and PG) were quantified by full scans in the negative ion mode. LPCs were quantified by detecting the *m/z* = 184 choline fragment ion through multiple reaction monitoring.

The cellular uptake of PC(16:0/20:4) was analyzed by multiple reaction monitoring (transition to 16:0 and 20:4 anions), and levels of free 20:4 were analyzed by single ion monitoring using a QTRAP 5500 Mass Spectrometer (AB Sciex). In variation to the settings described and referenced above, the ion spray voltage was set to 4,500 V in the negative ion mode, the heated capillary temperature was set to 500–700 °C, the sheath gas pressure was set to 45–60 psi, the auxiliary gas pressure was set to 75–85 psi, and the declustering potential was set to 45–50 V.

Mass spectra were processed using the Xcalibur 2.0 (Thermo Scientific) or Analyst 1.6 software (AB Sciex) as described (24).

Sample Preparation, SDS/PAGE, and Western Blot. Cells (0.5–2.0 \times 10⁶) were resuspended in 100 μ L lysis buffer [20 mM Tris-HCl, pH 7.4, 150 mM NaCl, 2 mM EDTA, 1% (vol/vol) Triton X-100, 1 mM phenylmethanesulphonyl fluoride, 60 μ g/mL soybean trypsin inhibitor, 10 μ g/mL leupeptin, 5 mM sodium fluoride, 1 mM sodium vanadate, and 2.5 mM sodium pyrophosphate]. After 5 min on ice, the lysate was sonified on ice (2 \times 5 s) and centrifuged (12,000 \times g, 5 min, 4 °C). The supernatant was analyzed for its protein concentration (DC protein Assay kit; Bio-Rad Laboratories), taken up in 1 \times SDS/PAGE sample loading buffer [125 mM Tris-HCl, pH 6.5, 25% (wt/vol) sucrose, 5% SDS (wt/vol), 0.25% (wt/vol) bromophenol blue, and 5% (vol/vol) β -mercaptoethanol], and boiled for 5 min at 95 °C. Aliquots (10 μ g protein) were resolved by 10% or 12% (wt/vol) SDS/PAGE and transferred to a Hybond ECL nitrocellulose membrane (GE Healthcare). After blocking with 5% (wt/vol) BSA or skim milk for 1 h at room temperature, membranes were washed and incubated with primary antibodies overnight at 4 °C. The membranes were washed again, and incubated with IRDye 800CW-labeled anti-rabbit, anti-mouse, or anti-goat IgG (1:10,000 each) and/or with IRDye 680LT-labeled anti-rabbit or anti-mouse IgG (1:80,000, each). Immunoreactive bands were visualized by an Odyssey infrared imager (LI-COR Biosciences). Data from densitometric analysis were background corrected.

Immunofluorescence Staining and Microscopy. NIH 3T3 cells were seeded onto poly-L-lysine-coated coverslips and cultured under the specified conditions at 37 °C and 5% CO₂. Cells were fixed with 4% paraformaldehyde in PBS-II (PBS, 0.1 mM CaCl₂, 1 mM MgCl₂) and permeabilized with 0.3% Triton X-100 in PBS-II. Samples were blocked with 5% normal goat serum for 60 min at room temperature, incubated with rabbit anti-Akt (1:100) for 2 h at room temperature, and then stained with goat anti-rabbit IgG Alexa Fluor 488 (1:500; 1 h, room temperature). The DNA was stained with 0.1 μ g/mL DAPI in PBS-II for 3 min at room temperature. The cells were mounted on glass slides in Mowiol solution and viewed using an Axio Observer Z1 microscope (Carl Zeiss). Control incubations lacking primary antibodies were routinely performed.

Determination of Cellular PIP₃ Levels. PIP₃ was extracted from NIH 3T3 cells and analyzed by a PIP₃ mass ELISA kit according to the manufacturer's instructions (Echelon Biosciences).

Cell-Free Akt Translocation Assay. Full-length nonactivated human Akt1 (1 μ g) was spotted onto nitrocellulose membranes. After blocking the membranes with PBS plus 3% (wt/vol) BSA (blocking buffer) for 1 h, they were treated with liposome suspensions (10 μ g/mL in blocking buffer) for another 1 h. Liposomes consisting of PC from egg yolk [0–68% (wt/vol)], PC(16:0/20:4) or PC(17:0/17:0) [0–68% (wt/vol)], PE(16:0/18:1) [29% (wt/vol)], *N*-biotinyl PE (18:1/18:1) [1% (wt/vol)], and 1,2-dioleoyl-*sn*-glycero-3-phosphatidylinositol-

3',4',5'-triphosphate [PIP₃(18:1/18:1), 2% (wt/vol)] were freshly prepared by sonication for 5 min at room temperature. After extensive washing with blocking buffer, bound liposomes were stained with IRDye 800CW-labeled streptavidin (1:2,000) and visualized by an Odyssey infrared imager (LI-COR Biosciences). Data from densitometric analysis were background corrected.

Statistics. Data are presented as mean ± SEM of *n* observations. Statistical evaluation of the data were performed by one-way ANOVAs for independent or correlated samples followed by Tukey HSD post hoc tests or by Student *t* test for paired and correlated samples. *P* < 0.05 was considered

statistically significant. All statistical calculations were performed using GraphPad InStat 3.10 (GraphPad Software).

ACKNOWLEDGMENTS. We thank Angela Herre for expert technical assistance with flow cytometric experiments. This work was supported by a Grant-in-Aid for Scientific Research (S) from the Ministry of Education, Culture, Sports, Science and Technology (MEXT) of Japan (to T.S.). H.S. was supported by a Grant-in-Aid for Young Scientists (B) from the MEXT of Japan and the Cell Science Research Foundation. A.K. received a stipend from the Takeda Science Foundation.

- Manning BD, Cantley LC (2007) AKT/PKB signaling: Navigating downstream. *Cell* 129(7):1261–1274.
- Ohira T, et al. (2010) Resolvin E1 receptor activation signals phosphorylation and phagocytosis. *J Biol Chem* 285(5):3451–3461.
- Hers I, Vincent EE, Tavaré JM (2011) Akt signalling in health and disease. *Cell Signal* 23(10):1515–1527.
- Shtivelman E, Sussman J, Stokoe D (2002) A role for PI 3-kinase and PKB activity in the G2/M phase of the cell cycle. *Curr Biol* 12(11):919–924.
- Lee SR, et al. (2005) Akt-induced promotion of cell-cycle progression at G2/M phase involves upregulation of NF-Y binding activity in PC12 cells. *J Cell Physiol* 205(2): 270–277.
- Gao N, Zhang Z, Jiang BH, Shi X (2003) Role of PI3K/AKT/mTOR signaling in the cell cycle progression of human prostate cancer. *Biochem Biophys Res Commun* 310(4): 1124–1132.
- Barré B, Perkins ND (2007) A cell cycle regulatory network controlling NF-kappaB subunit activity and function. *EMBO J* 26(23):4841–4855.
- Hermansson M, Hokynar K, Somerharju P (2011) Mechanisms of glycerophospholipid homeostasis in mammalian cells. *Prog Lipid Res* 50(3):240–257.
- Shindou H, Shimizu T (2009) Acyl-CoA:lysophospholipid acyltransferases. *J Biol Chem* 284(1):1–5.
- Jackowski S (1996) Cell cycle regulation of membrane phospholipid metabolism. *J Biol Chem* 271(34):20219–20222.
- Tercé F, Brun H, Vance DE (1994) Requirement of phosphatidylcholine for normal progression through the cell cycle in C3H/10T1/2 fibroblasts. *J Lipid Res* 35(12): 2130–2142.
- Lykidis A, Jackowski S (2001) Regulation of mammalian cell membrane biosynthesis. *Prog Nucleic Acid Res Mol Biol* 65:361–393.
- Manguikian AD, Barbour SE (2004) Cell cycle dependence of group VIA calcium-independent phospholipase A2 activity. *J Biol Chem* 279(51):52881–52892.
- Chen HH, Zhao S, Song JG (2003) TGF-beta1 suppresses apoptosis via differential regulation of MAP kinases and ceramide production. *Cell Death Differ* 10(5):516–527.
- Morgan DO (1995) Principles of CDK regulation. *Nature* 374(6518):131–134.
- Chang F, et al. (2003) Involvement of PI3K/Akt pathway in cell cycle progression, apoptosis, and neoplastic transformation: A target for cancer chemotherapy. *Leukemia* 17(3):590–603.
- Koeberle SC, et al. (2012) Skepinone-L is a selective p38 mitogen-activated protein kinase inhibitor. *Nat Chem Biol* 8(2):141–143.
- Murray AW (2004) Recycling the cell cycle: Cyclins revisited. *Cell* 116(2):221–234.
- Gijón MA, Riekhof WR, Zarini S, Murphy RC, Voelker DR (2008) Lysophospholipid acyltransferases and arachidonate recycling in human neutrophils. *J Biol Chem* 283(44):30235–30245.
- Shimizu T, Ohto T, Kita Y (2006) Cytosolic phospholipase A2: Biochemical properties and physiological roles. *IUBMB Life* 58(5-6):328–333.
- Shimizu T (2009) Lipid mediators in health and disease: Enzymes and receptors as therapeutic targets for the regulation of immunity and inflammation. *Annu Rev Pharmacol Toxicol* 49:123–150.
- Balsinde J, Winstead MV, Dennis EA (2002) Phospholipase A(2) regulation of arachidonic acid mobilization. *FEBS Lett* 531(1):2–6.
- Eling TE, Glasgow WC (1994) Cellular proliferation and lipid metabolism: Importance of lipoxygenases in modulating epidermal growth factor-dependent mitogenesis. *Cancer Metastasis Rev* 13(3-4):397–410.
- Koeberle A, Shindou H, Harayama T, Shimizu T (2012) Palmitoleate is a mitogen, formed upon stimulation with growth factors, and converted to palmitoleoyl-phosphatidylinositol. *J Biol Chem* 287(32):27244–27254.
- Whatley RE, Satoh K, Zimmerman GA, McIntyre TM, Prescott SM (1994) Proliferation-dependent changes in release of arachidonic acid from endothelial cells. *J Clin Invest* 94(5):1889–1900.
- Wang D, Dubois RN (2006) Prostaglandins and cancer. *Gut* 55(1):115–122.
- Nishiyama A, Cavagliere CR, Curi R, Calder PC (2000) Arachidonic acid-containing phosphatidylcholine inhibits lymphocyte proliferation and decreases interleukin-2 and interferon-gamma production from concanavalin A-stimulated rat lymphocytes. *Biochim Biophys Acta* 1487(1):50–60.
- Yang X, Sheng W, Sun GY, Lee JC (2011) Effects of fatty acid unsaturation numbers on membrane fluidity and α -secretase-dependent amyloid precursor protein processing. *Neurochem Int* 58(3):321–329.
- Wood R (1973) Lipids of cultured hepatoma cells. I. Effect of serum lipid levels on cell and media lipids. *Lipids* 8(12):690–701.
- Quehenberger O, et al. (2010) Lipidomics reveals a remarkable diversity of lipids in human plasma. *J Lipid Res* 51(11):3299–3305.
- Zaridze DG, Chevchenko VE, Levtschuk AA, Lifanova YE, Maximovitch DM (1990) Fatty acid composition of phospholipids in erythrocyte membranes and risk of breast cancer. *Int J Cancer* 45(5):807–810.
- Min HK, Lim S, Chung BC, Moon MH (2011) Shotgun lipidomics for candidate biomarkers of urinary phospholipids in prostate cancer. *Anal Bioanal Chem* 399(2): 823–830.
- Sutphen R, et al. (2004) Lysophospholipids are potential biomarkers of ovarian cancer. *Cancer Epidemiol Biomarkers Prev* 13(7):1185–1191.
- Patterson AD, et al. (2011) Aberrant lipid metabolism in hepatocellular carcinoma revealed by plasma metabolomics and lipid profiling. *Cancer Res* 71(21):6590–6600.
- Hilvo M, et al. (2011) Novel theranostic opportunities offered by characterization of altered membrane lipid metabolism in breast cancer progression. *Cancer Res* 71(9): 3236–3245.
- Bligh EG, Dyer WJ (1959) A rapid method of total lipid extraction and purification. *Can J Biochem Physiol* 37(8):911–917.
- Koeberle A, Shindou H, Harayama T, Shimizu T (2010) Role of lysophosphatidic acid acyltransferase 3 for the supply of highly polyunsaturated fatty acids in TM4 Sertoli cells. *FASEB J* 24(12):4929–4938.
- Koeberle A, Shindou H, Harayama T, Yuki K, Shimizu T (2012) Polyunsaturated fatty acids are incorporated into maturing male mouse germ cells by lysophosphatidic acid acyltransferase 3. *FASEB J* 26(1):169–180.